The Solar-B Mission and the Forefront of Solar Physics
ASP Conference Series, Vol. 325, 2004
T. Sakurai and T. Sekii, eds.

Small-Scale Solar Magnetic Elements: Simulations and Observations

Sami K. Solanki and Manfred Schüssler

Max Planck Institute for Solar System Research,[†]
37191 Katlenburg-Lindau, Germany

Abstract. Both the small-scale and large-scale properties of solar features, such as sunspots and the solar corona, are influenced strongly by the small-scale structure of the underlying magnetic field. Even some global properties of the Sun, such as variations of the Sun's irradiance, depend on the local properties of small-scale magnetic features. We briefly describe these dependences, as well as recent results concerning the small-scale magnetic elements deduced from radiation MHD simulations and spectropolarimetric observations. The simulations reproduce a number of sensitive observational tests and explain, e.g. why G-band images allow only a part of the magnetic flux to be identified.

1. Introduction

The interaction of convective motions, radiative cooling, and magnetic field in the solar surface layers leads to the formation of magnetic elements, concentrations of magnetic flux with kG field strengths located in the intergranular downflow lanes (Solanki 1993; Vögler & Schüssler 2003). The self-organization of the solar magneto-convection system to form small-scale magnetic elements is of intrinsic interest. In addition, they and the processes taking place in and around them also play an important role in defining larger-scale phenomena. Three examples of such phenomena driven or at least strongly affected by small-scale fields are considered here.

Sunspots: Many of the basic global properties of sunspots (their thermal structure, the presence of the Evershed effect etc.) are thought to be the result of the fine structure of the sunspot magnetic field.

Variations of total and spectral solar irradiance: Such variations are caused by the Sun's variable magnetic field, with sunspots producing a darkening and small-scales magnetic elements a brightening of the Sun as a whole. Hence, changes in solar irradiance, and in particular the spectral irradiance, depend directly on the detailed thermal structure of small-scale magnetic elements.

Coronal heating: Fine-scale structure in the coronal magnetic field, in particular current sheets, are important for energy dissipation and coronal heating. At the same time, the horizontal motions of photospheric magnetic elements inject further energy into the corona. The formation of current sheets is also driven by the footpoint motions of the field lines, i.e. the horizontal motion of the photospheric magnetic elements.

[†]Previously known as Max-Planck-Institute for Aeronomy

2. Sunspots

The large-scale properties of sunspots are still a promising topic of study, as new instrumental capabilities and novel or improved data analysis techniques allow fresh knowledge to be gleaned. For example, as heavily observed a quantity as the radial dependence of the magnetic field in a sunspot (Solanki, Rüedi, & Livingston 1992; Lites et al. 1993; Keppens & Martínez Pillet 1996; Westendorp Plaza et al. 2001; Mathew et al. 2003) has been improved and extended by, e.g. the inclusion of the magnetic canopy or the 3-D structure of the field (Westendorp Plaza et al. 2001; Mathew et al. 2003; cf. Rüedi, Solanki, & Livingston 1995; Penn & Kuhn 1995).

How are large-scale properties of sunspots driven by small-scale processes? Consider the brightness of the umbra. Sunspot umbrae are too warm and bright to be entirely heated by radiation. Efforts to understand the brightness of umbrae have therefore concentrated on magnetoconvection in one form or another. The theoretical studies of magnetoconvection of relevance to sunspots encompass simple mixing-length formulations (e.g. Deinzer 1965), 2-D incompressible and compressible simulations (e.g. Hurlburt & Toomre 1988; Hurlburt et al. 1989) and full 3-D compressible MHD simulations (e.g. Tao et al. 1998). Reviews are given by Weiss (2002) and Solanki (2003). One of the interesting results found by, e.g. Tao et al. (1998) is the segregation of magnetic field and convection. In particular they find within a region of strong field small patches of weaker field associated with hot upflowing gas. Such features bear some resemblance to umbral dots, small, often unresolved brightening found in the umbrae of most sunspots. Umbral dots had previously been identified with hot upflowing gas (Parker 1979; Choudhuri 1986). In this model the magnetic field and convection is completely segregated, and umbral dots are field-free intrusions into the umbra. This is probably too extreme a picture, as the more recent simulations suggest. The best observations have failed to reveal the significantly reduced field strength in umbral dots predicted by such models. However, this may be due to the fact that the measurements sample too high layers in the atmosphere where the field is already homogeneous (Degenhardt & Lites 1993).

Another example of small-scale processes affecting large-scale properties is the brightness of the penumbra. Here the problem is more severe, since the penumbra emits roughly 75 % of the heat flux of the quiet Sun, and the magnetic structure is more complex, with the field being uncombed on a small scale (e.g. Degenhardt & Wiehr 1991; Title et al. 1993). Current thinking is that thin nearly horizontal magnetic flux tubes are embedded in an inclined background magnetic field (Solanki & Montavon 1993).

Given this complexity, it is not surprising that no real concensus has as yet been reached on the processes acting within a penumbra. Various proposals have been made. Convective rolls, i.e. rolling motions along a horizontal axis parallel to the horizontal component of the field, are the main source of energy transport according to one proposal (Danielson 1961). It works best if the penumbra is a shallow phenomenon, with field-free gas not far below the surface. However, Solanki & Schmidt (1993) have argued that the penumbra is deep, so that this process cannot act efficiently. In the interchange convection model (Schmidt 1991; Jahn & Schmidt 1994), whole flux tubes are heated at the subsurface magnetopause and rise to the solar surface, carrying heat with

them. After cooling by radiative losses at the solar surface they sink back to the magnetopause. As Solanki & Rüedi (2003) have pointed out, the magnetic and brightness structure of sunspots is rather stable, so that the interchange must happen at very small scales. It then becomes difficult to transport a sufficient amount of energy.

The Evershed flow itself carries considerable heat flux. This would suffice to heat the penumbra if the tubes carrying the flow have the form of a sea serpent, i.e. periodically dip below the surface (Schlichenmaier & Solanki 2003). Whether such a structure is present is currently uncertain. However diverse the above proposals may be, they have in common that the heat transport is governed by processes related to the small-scale structure of the magnetic field.

3. Solar Irradiance Variations: the Physics of Magnetic Elements

The Sun is a variable star at all wavelengths and its total irradiance (i.e. the wavelength-integrated radiation reaching the top of the Earth's atmosphere) varies by approximately 0.1% in phase with the solar cycle and shows larger amplitude excursions on a solar rotation time scale (e.g. Fröhlich 2003). These shorter-term dips are produced when a sunspot group passes over the solar surface, while the longer-term changes are largely caused by the change in the number of small-scale magnetic elements over the solar cycle (Krivova et al. 2003). What causes sunspots to block the heat flux and thus to darken the Sun? And which process is responsible for magnetic elements to enhance the heat flux and brighten the Sun? Owing to the strong magnetic field in sunspots (and in magnetic elements) convection, the main source of energy transport below the solar surface, acts far less efficiently within them (see Sect. 2), making them dark. One important feature underlying these processes is that the solar convection zone can be considered to be a nearly ideal reservoir of heat (possessing both high thermal conductivity and large heat capacity). This implies that any heat blocked by sunspots is quickly distributed throughout the convection zone (Spruit 1982). Similarly, any excess energy radiated by small scale magnetic elements is also replenished from the whole convection zone.

This by itself does not explain why magnetic elements are bright. In fact, the brightness of a magnetic element is produced by a delicate balance between a darkening due to the inhibition of convective motions within the magnetic elements and a brightening due to partial evacuation, which leads to enhanced transparency, so that hotter and brighter layers become visible, in particular the hot walls of magnetic elements radiating copiously. At the same time, the radiation flowing through these hot walls is channeled from the immediate surroundings, which get cooled. So what is the net effect? How bright are magnetic elements really? This question is not trivial to answer observationally since measurements are required at all wavelengths and at all limb distances for many different magnetic elements. One way to address it is to consider simulations of as high a degree of realism as possible and to carry out 'ideal' observations of this data set, once the results of the simulations have been validated against a wide variety of other observed quantities.

The simulations discussed here are 3-D, compressible MHD simulations with the effects of partial ionization and non-grey radiative transfer taken into ac-

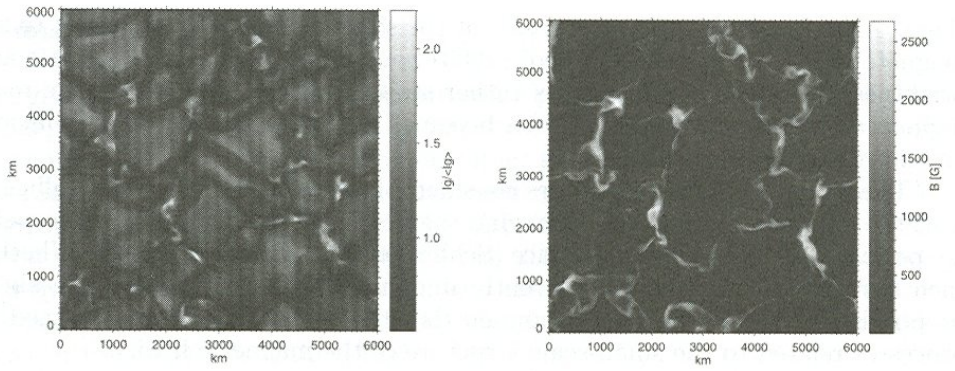

Figure 1. Simulated images of the G-band contrast (local G-band brightness divided by spatial average, $I_g/\langle I_g \rangle$), and magnetic structure at the solar surface. *Left*: Synthetic filter image of the simulation area (6000 × 6000 km^2) in the G-band spectral region around 430 nm. The extended bright regions are convective upwellings (granules) surrounded by a network of dark downflow lanes. The small brilliant patches in the dark areas coincide with magnetic flux concentrations. *Right*: Gray shading of the magnetic field strength (in units of Gauss) simultaneous to the G-band contrast image. About two-thirds of the vertical magnetic flux penetrating the simulation box has been assembled into flux concentrations with a field strength above 1000 G (100 mT). Figure from Schüssler et al. (2003).

count. A box with the dimensions 6 × 6 × 1.4 Mm is considered. The average solar surface (τ=1 level) lies about 800 km above the bottom of the box. Further details on the code, the simulation runs etc. are given by Vögler (2003) and Vögler & Schüssler (2003).

A sensitive probe of the temperature structure of the lower and middle photosphere is the G-band brightness, which is now widely used to trace small-scale magnetic elements (see paper by Berger & Title (2004) in these proceedings and references therein). The simulations described above have therefore been used to produce synthetic G-band images. A spectral synthesis, including 87 atomic and 241 CH lines, is carried out between 4295 Å and 4315 Å, for each pixel of a snapshot. Finally, the computed spectrum is multiplied with an appropriate filter function and spectrally integrated.

In Fig. 1 a snapshot of the G-band contrast (left) and the magnetic field strength (right) are plotted for a simulation starting with a vertical field of 200 G everywhere. It is evident that the magnetic field gets concentrated into the dark downflow lanes, where field strengths in excess of 1500 G at the solar surface are common. The field forms sheet-like structures, reminiscent of the magnetic flux sheets studied by Deinzer et al. (1984), Knölker, Schüssler, & Weisshaar (1988), and Grossmann-Doerth et al. (1994). Not only is the field concentrated by the convection, but the concentrated field also affects the convection, in particular the intergranular lanes: at locations of strong field the lanes are brighter and the downflows are quenched or at least strongly reduced. The synthetic G-band images show the magnetic elements as thin bright threads within the intergranular lanes (Schüssler et al. 2003; Shelyag et al. 2004).

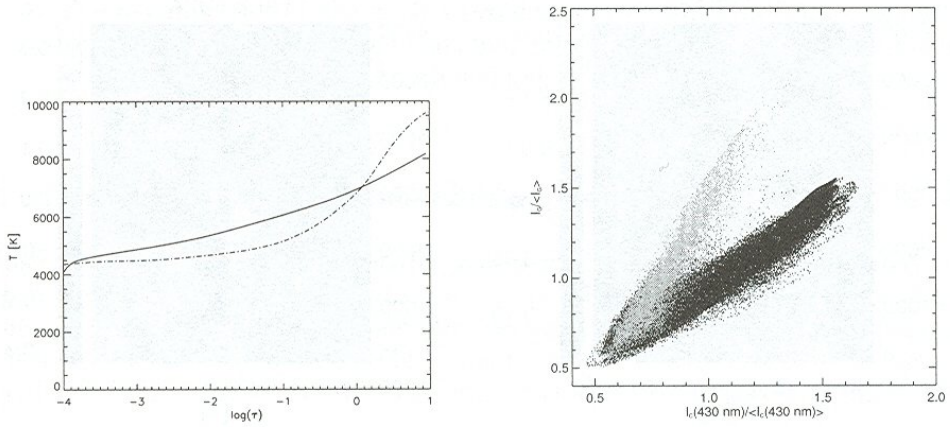

Figure 2. *Left*: Average temperature profiles from the simulation run with 200 G average vertical field. The solid curve shows the magnetic component ($B > 1000$ G) while the dash-dotted line represents the largely nonmagnetic granules ($B < 100$ G). *Right*: Scatter diagram of G-band contrast vs. 430 nm continuum contrast. The black points correspond to weakly magnetic regions ($B < 500$ G) while the grey points correspond to flux concentration ($B > 500$ G).

Although at equal geometrical height the magnetic features generally somewhat cooler than their surroundings, at equal optical depth the magnetic features are significantly hotter than the field-free regions due to the partial evacuation. This is illustrated in the left frame of Fig. 2 (from Shelyag et al. 2004), which shows the temperature stratifications averaged over all pixels with $B > 1000$ G (solid curve) and $B < 100$ G (dot-dashed curve). In the mid photosphere the magnetic features are on average 800 K hotter, while becoming cooler below roughly the τ=1 level. This agrees reasonably well with the empirical models of Solanki & Brigljević (1992). The simulations deviate significantly from the empirical models in the upper photosphere (see Briand & Solanki 1995). We expect this to be due to the upper boundary condition.

When the G-band brightness is plotted vs. continuum intensity (see the right frame of Fig. 2) the magnetic features exhibit a steeper dependence (G-band brightness increases more rapidly than continuum brightness) than the pixels associated with little field (G-band intensity increases less rapidly than continuum intensity). Figure 2 not only reveals why many magnetic features are so easily visible in the G-band. It also identifies many points with simultaneously large field and low G-band brightness. These points are difficult to identify as magnetic purely on the basis of G-band intensity.

A comparison of simulated G-band brightness (after appropriate spatial smearing) with observations obtained with the SST of a region that appears to contain roughly the same amount of magnetic flux (Scharmer et al. 2002) reveals considerable similarity between the two in a statistical sense. A more quantitative comparison based on the Probability Distribution Function (PDF) confirms this similarity with remarkable accuracy.

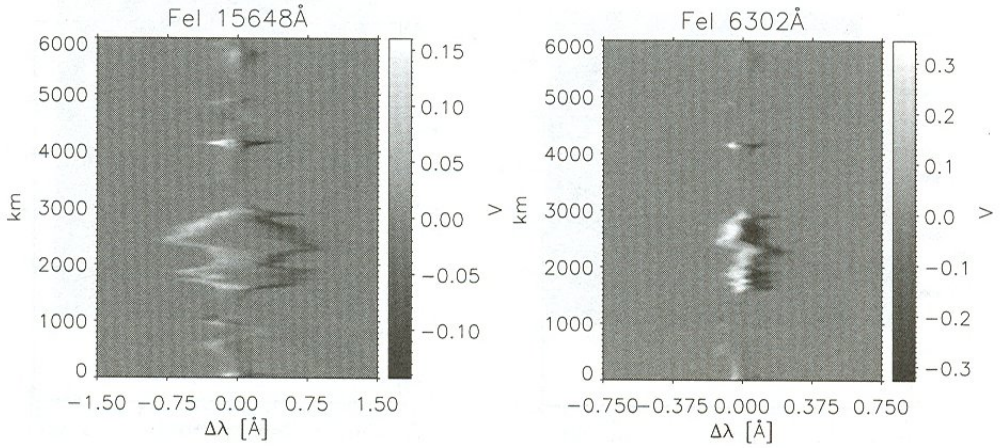

Figure 3. Synthetic slit spectra of Stokes V from the simulation. *Left*: Fe I 15648 Å, *right*: Fe I 6302 Å.

Further information can be gleaned from the computation of the Stokes parameters of Zeeman-sensitive lines. The Stokes V profile of the very Zeeman sensitive Fe I line at 1.5648 μm formed along an artifical slit laid through a snapshot of the simulations is illustrated in Fig. 3 (left frame), and of the Fe I 6302.5 Å line in Fig. 3 (right frame). The extreme Zeeman sensitivity of the IR line is amply demonstrated by the figure. This sensitivity not only produces the large splitting in concentrated magnetic features, but also produces an appreciable Zeeman signal also at locations with weak fields. The visible line exhibits a large contrast in the Stokes V profile amplitudes from the pixels with strong and weak fields. A detailed analysis of such spectra, of the underlying atmospheres and the comparison with observational results after appropriate smearing leads to numerous insights. For example:

1. The internal structure of small-scale magnetic features in the 3-D simulations is similar to magnetic flux sheets that satisfy the thin-tube approximation (Defouw 1976).
2. Over a large range of field strengths, the observed and simulated Probability Distribution Function (PDF) of the field strength for the quiet Sun is close to an exponential function (Khomenko et al. 2003; Vögler & Schüssler 2003). This means that a significant fraction of the magnetic flux is in weak-field form. To what extent such fields are turbulent needs to be investigated. Sánchez Almeida, Domínguez Cerdeña, & Kneer (2003) find indications of a super-exponential tail of the PDF in the kG range by combining spectral line observations in the infrared and the visible.
3. Owing to the differences in magnetic sensitivity, spatial smearing and noise have rather different effect on IR and visible lines (Socas Navarro & Sánchez Almeida 2002, 2003). Nonetheless, it is possible with both to deduce the true PDF of the magnetic field if sufficient care is taken with the analysis (Khomenko et al., in preparation).

4. The asymmetries of the Stokes profiles provide an important diagnostics for the fine-scale structure of the magnetic field (e.g. Solanki 1993; Solanki & Montavon 1993; Sánchez Almeida et al. 1996).

4. Coronal Heating and Small-Scale Magnetic Fields

Basically two types of field lines are present in the solar corona, associated with open and closed flux, the latter forming loops. The source of both types of field lines are magnetic fibrils or magnetic elements in the photosphere, which are affected by convective motions. These motions lead to braiding of field lines and to the formation of tangential discontinuities or current sheets (Parker 1983,

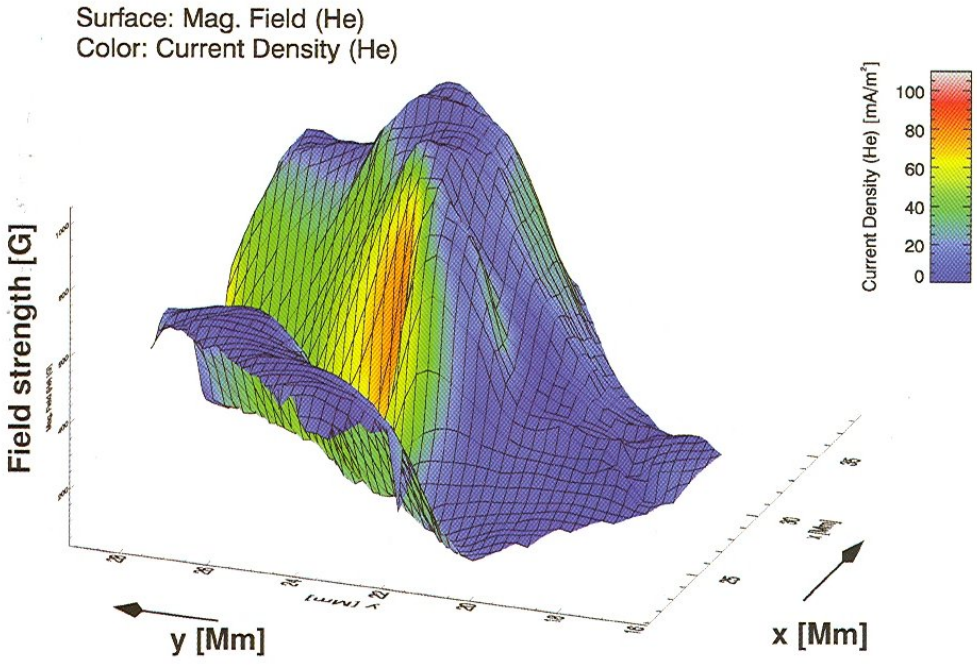

Figure 4. Representation of an electric current sheet near the base of the corona. The elevation of the meshed surface is proportional to the magnetic field strength in the upper chromosphere. A narrow valley of low magnetic field values separates two areas of opposite magnetic polarity, so that an electric current flows along this boundary parallel to the solar surface. The color-coding in the figure indicates the current density of this current sheet calculated using Ampére's Law. The maximum value of approximately 90 $\mathrm{mA/m^2}$ in the region of the largest magnetic field gradient perpendicular to the current sheet represents only a lower limit of the actual current flowing in this chromospheric current sheet. The width of the valley in the magnetic field strength corresponds to the spatial resolution of 1 Mm, limited by turbulence in the Earth's atmosphere, so that the horizontal gradient of the magnetic field is underestimated (from Solanki et al. 2003).

1988) along which magnetic energy can be converted into kinetic energy of the gas through reconnection or thermal energy through Ohmic dissipation.

Many examples of the rearrangement of coronal structures that can be interpreted in terms of magnetic reconnection have been provided by Yohkoh (Acton et al. 1992). Its superior spatial resolution and the possibility to combine X-ray, EUV and spectropolarimetric data will allow Solar-B to go well beyond what was possible with Yohkoh. It awaits to be seen if signatures of reconnection as clear cut as that found by SUMER for transition-region explosive events (Innes et al. 1997) will also be found for the coronal plasma.

Until recently, the presence of current sheets had only been deduced indirectly, the main difficulty being that it is necessary to deduce both the strength and direction of the field at high spatial resolution. The ability to record the full Stokes vector in the He I 10830 Å triplet with the Tenerife Infrared Polarimeter opens up the possibility to detect such a current sheet. The He I triplet, although not a coronal line, is formed near the base of the corona where the magnetic field has expanded, so that it fills all of space. Therefore, current sheets are expected to be more common than in deeper layers. Indeed, the very first map of the full magnetic vector made in an emerging active region revealed the presence of such a current sheet (Solanki et al. 2003; cf. Lagg et al. 2004).

The field strength in a rectangular box along an abrupt jump in inclination of the field is shown in Fig. 4 (vertical axis). Remarkable is the deep valley, with a width corresponding to the spatial resolution element of the observations (suggesting that it is spatially unresolved). It marks the boundary between the opposite polarities and hence the location of the current sheet. The current density values are indicated by the shading in Fig. 4.

5. Conclusion

The rich magnetic fine structure of the Sun, often unresolved in current observations, is a key ingredient of many solar phenomena. One of the major hurdles to a better knowledge of small-scale magnetic features is limitations in spatial resolution besetting current observations. The highest spatial resolution reached by current magnetogram is roughly 200–250 km. In contrast, the simulations described in Sect. 3 have a "spatial resolution", i.e. 2 grid points, of roughly 40 km. It is quite obvious from Fig. 1 that there are many magnetic features in the simulations that are significantly narrower than 250 km and cannot be resolved by current measurements. Needed are seeing-free high-resolution time series of magnetograms and spectropolarimetric data. Exactly such data will be provided by Solar-B and we expect significant progress towards resolving many important open questions from the visible light Solar-B data. They should help answer questions such as the following: Which fraction of the magnetic flux is in the form of kG fields in the quiet Sun? Which is the main energy transport mechanism in the penumbrae of sunspots? How large are the horizontal motions of magnetic elements (i.e. footpoint motions of magnetic loops) and what spectrum do they follow?

In spite of the huge expected impact of Solar-B, some questions will perforce remain unanswered. One reason for this can be seen from Fig. 1. Many of the magnetic features in the simulations are so narrow that they are also well

below the spatial resolution of Solar-B (140–150 km), so that even higher spatial resolution is required. This will hopefully be provided by the Sunrise project (Solanki et al. 2001) whose aim is to observe the Sun at the highest possible spatial resolution in order to precisely determine areas in which our knowledge is incomplete and where improvements in the simulations are necessary. To achieve this aim a 1-m diameter telescope with a spectropolarimeter, a magnetograph and a UV imager will be launched with a balloon into the antarctic stratosphere. Of particular interest will be possible parallel observations made by Solar-B and Sunrise since the two projects complement each other in many ways.

References

Acton, L., & 9 co-authors 1992, Sci, 258, 618.

Berger, T. E., & Title, A. M. 2004, in ASP. Conf. Ser., 325, The Solar-B Mission and the Forefront of Solar Physics: The Fifth Solar-B Science Meeting, ed. T. Sakurai & T. Sekii (San Francisco: ASP), 95

Briand, C., & Solanki, S. K. 1995, A&A, 299, 596

Choudhuri, A. R. 1986, ApJ, 302, 809

Danielson, R. E. 1961, ApJ, 134, 289

Defouw, R. J. 1976, ApJ, 209, 266

Degenhardt, D., & Lites, B. W. 1993, ApJ, 416, 875

Degenhardt, D., & Wiehr, E. 1991, A&A, 252, 821

Deinzer, W. 1965, ApJ, 141, 548

Deinzer, W., Hensler, G., Schüssler, M., & Weisshaar, E. 1984, A&A, 139, 435

Fröhlich, C. 2003, in Solar Variability as an Input to the Earth's Environment, ed. A. Wilson (ESA SP-535), 183

Grossmann-Doerth, U., Knölker, M., Schüssler, M., & Solanki S. K. 1994, A&A, 285, 648

Hurlburt, N. E., & Toomre, J. 1988, ApJ, 327, 920

Hurlburt, N. E., Proctor, M. R. E., Weiss, N. O., & Brownjohn, D. P. 1989, J. Fluid Mech., 207, 587

Innes, D. E., Inhester, B., Axford, W. I., & Wilhelm, K. 1997, Nat, 386, 811

Jahn K., & Schmidt, H. U. 1994, A&A, 290, 295

Keppens, R., & Martínez Pillet, V. 1996, A&A, 316, 229

Khomenko, E. V., Collados, M., Solanki, S. K., Lagg, A., & Trujillo Bueno, J. 2003, A&A, 408, 1115

Knölker, M., Schüssler, M., & Weisshaar, E. 1988, A&A, 194, 257

Krivova, N. A., Solanki, S. K., Fligge, M., & Unruh, Y. C. 2003, A&A, 399, L1

Lagg, A., Woch, J., Krupp, N., & Solanki, S. K. 2004, A&A, 414, 1109

Lites, B. W., Elmore, D. F., Seagraves, P., & Skumanich, A. P. 1993, ApJ, 418, 928

Mathew, S. K., & 8 co-authors 2003, A&A, 410, 695

Parker, E. N. 1979, Cosmical Magnetic Fields (Oxford: Clarendon Press)

Parker, E. N. 1983, ApJ, 264, 642

Parker, E. N. 1988, ApJ, 330, 474

Penn, M. J., & Kuhn, J. R. 1995, ApJ, 441, 51

Rüedi, I., Solanki, S. K., & Livingston, W. C. 1995, A&A, 293, 252

Sánchez Almeida, J., Domínguez Cerdeña, I., & Kneer, F. 2003, ApJ, 597, L177

Sánchez Almeida, J., Landi degl'Innocenti, E., Martinez Pillet, V., & Lites, B. W. 1996, ApJ, 466, 537

Scharmer, G., Gudiksen, B. V., Kiselman, D., Löfdahl, M. G., & Rouppe van der Voort, L. H. M. 2002, Nat, 420, 151

Schlichenmaier, R., & Solanki, S. K. 2003, A&A, 411, 257

Schmidt, H. U. 1991, Geophys. Astrophys. Fluid Dyn., 62, 249

Schüssler, M., Shelyag, S., Berdyugina, S., Vögler, A., & Solanki, S. K. 2003, ApJ, 597, L173

Shelyag, S., Schüssler, M., Solanki, S. K., Berdyugina, S., & Vögler, A. 2004, A&A, 427, 335

Socas Navarro, H., & Sánchez Almeida, J. 2002, ApJ, 565, 1323

Socas Navarro, H., & Sánchez Almeida, J. 2003, ApJ, 593, 581

Solanki, S. K. 1993, Space Sci. Rev., 63, 1

Solanki, S. K. 2003, A&A Rev., 11, 153

Solanki, S. K., & Brigljević, V. 1992, A&A, 262, L29

Solanki, S. K., Lagg, A., Woch, J., Krupp, N., & Collados, M. 2003, Nat, 425,692

Solanki, S. K., & Montavon, C. A. P. 1993, A&A, 275, 283

Solanki, S. K., & Rüedi, I. 2003, A&A, 411, 249

Solanki, S. K., Rüedi, I., & Livingston, W. 1992, A&A, 263, 339

Solanki, S. K., & Schmidt, H. U. 1993, A&A, 267, 287

Spruit, H. C. 1982, A&A, 108, 356

Tao, L., Weiss, N. O., Brownjohn, D. P., & Proctor, M. R. E. 1998, ApJ, 496, 39

Title, A. M., Frank, Z. A., Shine, R. A., Tarbell, T. D., Topka, K. P., Scharmer, G., & Schmidt, W. 1993, ApJ, 403, 780

Vögler, A. 2003, Three-Dimensional Simulations of Magneto-Convection in the Solar Photosphere, Ph. D. Thesis, University of Göttingen

Vögler, A., & Schüssler, M. 2003, Astron. Nachr., 324, 399

Weiss, N. O. 2002, Astron. Nachr., 323, 371

Westendorp Plaza, C., del Toro Iniesta, J. C., Ruiz Cobo, B., Martinez Pillet, V., Lites, B. W., & Skumanich, A. 2001, ApJ, 547, 1130